Fundamental and environmental contributions to the cyclostationary third moment of current fluctuations in a tunnel junction

Pierre Février, Christian Lupien, and Bertrand Reulet
Institut Quantique and Département de Physique, Université de Sherbrooke, Sherbrooke, Québec, Canada J1K 2R1

(Received 12 February 2020; revised manuscript received 29 May 2020; accepted 29 May 2020; published 29 June 2020)

Current fluctuations generated by tunnel junctions are known to be non-Gaussian. However, this property is lost when fluctuations are measured at high frequency and limited bandwidth. We show that the fluctuations of the electric field generated by a tunnel junction at frequency f displays third order correlations, i.e., skewness, when the junction is electrically driven at $3f$, revealing the Poisonnian statistic of charge transfer by the barrier even at short timescales. In addition to this intrinsic contribution from the junction, we observe extra correlations induced by the environmental noise at frequency f as well as a feedback effect coming from the environmental impedance not only at frequency f but also at some multiples of f.

DOI: 10.1103/PhysRevB.101.245440

I. INTRODUCTION

Electronic noise in mesoscopic conductors has been the object of many investigations [1]. Indeed, quantum transport is determined by the statistics, dynamics, and interactions of charge carriers. These are imprinted in the statistics of current fluctuations, the study of which thus provides insights into the conduction mechanisms. Many experiments deal with the variance of voltage or current fluctuations, measured over long timescales, i.e., at low frequency, which already provides interesting information beyond the measurement of the conductance. However, in order to access dynamical properties, it is usually necessary to perform detection at shorter timescales, i.e., to work at finite frequency f. Unfortunately, the variance of fluctuations, which is the simplest quantity to measure beyond average current, is usually frequency independent when charge is conserved [2]. Beyond the variance, the noise susceptibility, i.e., the dynamical response of noise to an ac excitation, has proven to be a probe of the energy relaxation time in wires [3,4]. Photoassisted noise can also be used to access the same quantity [5].

Beyond usual variance, higher order moments have been measured in various samples [6,7]. For systems with slow dynamics like quantum dots, frequency-dependent statistics reveal the tunnel rates through the barriers [8,9]. In samples with fast dynamics such as metallic wires [10–12], the frequencies involved are in the GHz range, and microwave techniques are mandatory. The third moment of current fluctuations in such a frequency domain has been performed in tunnel junctions [13] and short diffusive wires [14]. These experiments face, beside the very low signal, two difficulties: first, the need for a very wide bandwidth, which is difficult to achieve in microwave circuits. Second, it involves environmental contributions which arise as soon as the impedance of the detecting apparatus is nonzero [15]. In practice, this impedance is usually 50 Ω and of the same order as that of the sample. As a consequence, there is no report of detection of third order fluctuations in mesoscopic devices beyond 1 GHz, except by a mixed detection which involves both low and high frequencies [16,17].

The constraint on the detection bandwidth is stringent: A signal in the range $[f_1, f_2]$ has no third moment if $f_2 < 2f_1$, so for example, experiments working with a 4–8 GHz bandwidth, common in the detection of cryogenic microwave signals, are useless for the detection of a third moment. This severe condition originates from stationary: The third moment in frequency domain $\langle i(f_1)i(f_2)i(f_3)\rangle$ is zero unless $f_1 + f_2 + f_3 = 0$. This condition can be relaxed into $f_1 + f_2 + f_3 = nf_0$ with n any integer if the system is excited by a periodic signal at frequency f_0. This condition of cyclostationarity can be obeyed with a detector of narrow bandwidth for $n = \pm 1$, $f_0 = f$, to give the cyclic moment $K_1(f) = \langle i^2(f)i(-f)\rangle$, or for $f_0 = 3f$, to give the cyclic moment $K_3(f) = \langle i^3(f)\rangle$. Under cyclostationary conditions, a third moment of current fluctuations can in principle be measured with a narrow bandwidth detection scheme. The purpose of this paper is to implement such a measurement to address the second difficulty related to measurements of third moments in the microwave domain: What are the environmental effects in this measurement? This question has been partially addressed theoretically [18].

This communication is organized as follows: In Sec. II we describe the experimental setup and results of the measurement of the cyclostationary third moment of voltage fluctuations generated by a tunnel junction placed at low temperature; in Sec. III we analyze the results in terms of intrinsic contributions and environmental effects. Section IV contains a conclusion, remarks, and perspectives.

II. EXPERIMENTAL SETUP

A. Sample and biasing

Tunnel junctions are known to produce non-Gaussian fluctuations due to the binomial statistics of the charge transfer through the tunneling barrier. We used a junction similar to the ones used in shot-noise thermometry [19], with a

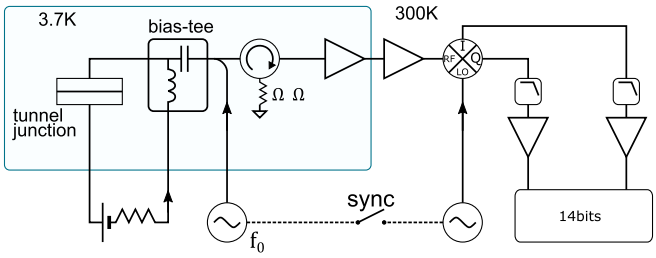

FIG. 1. Experimental setup. The sample is excited at frequency $f_0 = 3f = 14.55$ GHz. The LO of the IQ mixer is at frequency $f = 4.85$ GHz.

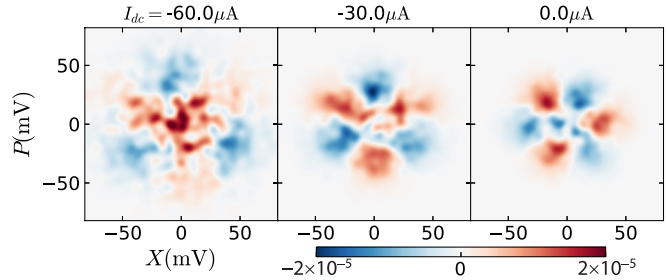

FIG. 2. Differential probability density $\Delta\mathcal{P}(X, P)$ of the in-phase and in-quadrature components of voltage fluctuations at frequency $f = 4.85$ GHz generated by a tunnel junction under cyclostationary excitation at frequency $3f$ (after subtraction of the phase insensitive contributions). The existence of a third order moment is revealed by the rotational symmetry clearly visible in the data. Different plots correspond to different dc biases.

planar geometry of area 5×1 μm. It has been made using usual lithography techniques and evaporation of aluminum electrodes on a silicon substrate. The insulating tunnel barrier is obtained by controlled oxidation of the first electrode under oxygen atmosphere. The dc resistance of the junction is $R_J = 130$ Ω at 3.7 K (116 Ω at 300 K). The experiment has been performed in a helium-free cryostat with a base temperature of 3.7 K so that aluminum is not superconducting. The junction is current biased through a bias-Tee (see Fig. 1), allowing the separation of high frequency signals from the dc bias line. The junction is ac biased by a single tone at frequency $f_0 = 3f = 14.55$ GHz using a directional coupler.

B. Homodyne measurement

The spectral density of voltage fluctuations at the junction is of the order of 10^{-10} V/$\sqrt{\text{Hz}}$ which is way too small for direct detection without amplification. The microwave signal generated by the junction propagates through an isolator before amplification by a low-noise 4–8 GHz cryogenic amplifier with a noise temperature of 2.5 K. The role of the isolator is to make the temperature and the impedance of the environment seen by the junction well defined: a 50 Ω load at 3.7 K instead of the input of the amplifier with an unknown, frequency-dependent impedance and noise temperature. After extra amplification at room temperature, the signal is down-converted from $f = 4.85$ GHz to low frequency by an IQ mixer with high linearity. The in-phase and in-quadrature components X and P are amplified and low-pass filtered, with a measurement bandwidth of $\Delta f = 225$ MHz. The signal is then digitized with a fast acquisition card (14 bits, 400 MS/s). The joint probability density $\mathcal{P}(X, P)$ is calculated on the fly from the acquired data. The skewness of the voltage fluctuations $\langle X^3\rangle$ and $\langle P^3\rangle$ is directly linked to the cyclic third moments $K_{v,3}(f) = \langle v_{\text{mes}}(f)^3\rangle$ and $K_{v,1}(f) = \langle v_{\text{mes}}(f)^2 v_{\text{mes}}(-f)\rangle$ of voltage fluctuations $v_{\text{mes}}(f)$ measured at the input of the cryogenic amplifier:

$$\langle X^3\rangle + i\langle P^3\rangle = \tfrac{3}{4}G^3[K_{v,3}(f)e^{i3\phi_0} + 3K_{v,1}(f)e^{i\phi_0}]\Delta f^2, \quad (1)$$

where G is the total voltage gain of the amplification chain and ϕ_0 a global phase due to the delay between excitation and detection. The amplitude of the ac excitation I_{ac}, the gain G, and the noise added by the amplification chain are calibrated by measuring the variance of the photoassisted noise $\langle X^2\rangle$ and $\langle P^2\rangle$ vs I_{dc}, the theory of which is well established [20,21]. The power gain G^2 is estimated around 78 dB and the effective noise temperature of the measurement is 3 K, as expected for a 130 Ω load with this specific cryogenic amplifier. The signal to noise ratio at high bias is limited by the noise of the junction itself.

C. Third moment from the symmetries of the histograms

The phase coherence between the detection at frequency f and the excitation at frequency $3f$ can be switched on or off. When off, a slight detuning of one of the microwave sources averages to zero the contributions that depend on ϕ_0 and thus should lead to $\langle X^3\rangle = 0$ and $\langle P^3\rangle = 0$. All remaining contributions are due to the nonlinearity of the amplification chain and of the acquisition card. To remove these unwanted contributions in $\mathcal{P}(X, P)$, we measure the difference in histograms obtained with and without phase coherence. The resulting differential probability $\Delta\mathcal{P}(X, P)$ showed Fig. 2 has a finite order rotational symmetry. This is the direct consequence of the homodyne demodulation of the noise at a fraction of the modulation frequency. It is then natural to write $\mathcal{P}(X, P)$ in polar coordinates: $X = r\cos\theta$ and $P = r\sin\theta$ and express $\mathcal{P}(r, \theta)$ as the Fourier series:

$$\mathcal{P}(r, \theta) = \sum_{n\in\mathbb{Z}} \mathcal{P}_n(r)e^{-in\theta}. \quad (2)$$

We define:

$$W_{\alpha,n} = \frac{\pi}{2}\int_0^{+\infty} \mathcal{P}_n(r)r^{\alpha+1}dr. \quad (3)$$

Moments of the probability distribution $\mathcal{P}(X, P)$ are related to the $W_{\alpha,n}$, which can be interpreted as the contribution of the rotational symmetry of order n to the moment of order α. For the third moment we find:

$$\begin{aligned}\langle X^3\rangle &= \text{Re}(W_{3,3} + 3W_{3,1})\\ \langle XP^2\rangle &= \text{Re}(W_{3,1} - W_{3,3})\\ \langle P^3\rangle &= \text{Im}(W_{3,3} - 3W_{3,1})\\ \langle PX^2\rangle &= \text{Im}(W_{3,1} + W_{3,3}).\end{aligned} \quad (4)$$

The skewness of the marginal probability distributions $\mathcal{P}(X)$ and $\mathcal{P}(P)$ is finite when $\mathcal{P}(X, P)$ shows either a onefold

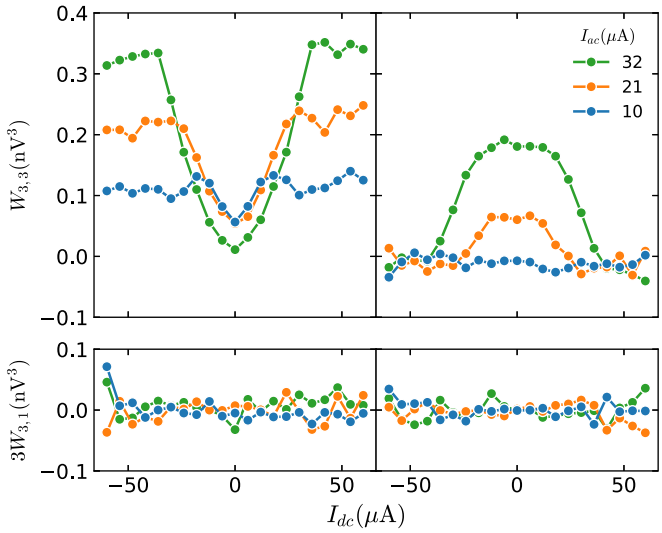

FIG. 3. Contributions $W_{3,3}$ and $W_{3,1}$ to the third moment of voltage fluctuations as a function of I_{dc} for various ac excitations. They are calculated using Eq. (3) from the measurements of the differential probability density $\Delta\mathcal{P}(X,P)$ of Fig. 2. The distributions $\mathcal{P}(X,P)$ have been rotated by a global angle in order to maximize the signal at high dc bias on the in-phase component X. Each data point is averaged over 45 mn.

or threefold symmetry characterized, respectively, by $W_{3,1}$ and $W_{3,3}$. The measurement of the joint probability is necessary to separate these two contributions. In our experiment, it appears that $W_{3,1} \simeq 0$ (see Fig. 3). This corresponds to $K_{v,1} = 0$ as expected for a modulation at frequency $3f$. We consider in the following $\langle X^3\rangle = \mathrm{Re}(W_{3,3})$ and $\langle P^3\rangle = \mathrm{Im}(W_{3,3})$, in order to improve signal to noise ratio, and an arbitrary phase ϕ_0 that maximizes $\langle X^3\rangle$ and makes $\langle P^3\rangle$ vanish at high bias.

From Fig. 3, we see that the measured third moment at high bias ($I_{dc} > 40\ \mu$A) shows a plateau with an amplitude proportional to I_{ac}. This is qualitatively close from what is expected for a tunnel junction, i.e., a third moment proportional to the average current $\langle I\rangle$: $\langle (I - \langle I\rangle)^3\rangle = e^2\langle I\rangle$ [6,22]. In the limit where the noise is adiabatically modulated, all the moments of the current distribution follow the bias modulation, and we should have $K_{v,3} \propto e^2 I_{ac}$. The third moment at low bias shows, however, a clear deviation from this behavior. In the following we show that there are extra contributions that comes from the measurement setup and demonstrate how to separate them.

III. EFFECT OF THE ENVIRONMENT

Ideally, current fluctuations in a conductor should be measured using a ammeter with both a fast response and a zero input impedance. However, microwave equipment has a 50 Ω input impedance. Furthermore, the tunnel junction is embedded in an electromagnetic environment consisting of its own capacitance, connecting leads, wire bonds, and a transmission line (TL). This can be modeled by the effective reciprocal circuit shown in Fig. 4. The input impedance Z_{in} represents the impedance seen by the junction, the output impedance Z_{out}, the effective load on the TL. The voltage transmission coefficients t(resp. t'), from the junction to the TL (resp. the TL to the junction), include the finite propagation time in the

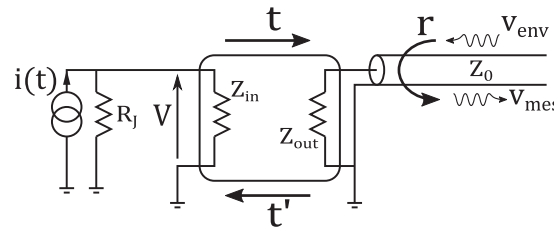

FIG. 4. Model for the impedance mismatch between the junction and the transmission line. The box represents an effective four ports circuit.

circuit. This environment induces voltage fluctuations across the junction given by:

$$\delta V(f) = -i(f)Z_{\mathrm{eff}}(f) + t'(f)v_{\mathrm{env}}(f) \tag{5}$$

with $Z_{\mathrm{eff}} = R_J Z_{\mathrm{in}}(f)/(R_J + Z_{\mathrm{in}}(f))$. v_{env} is the noise coming from the measurement setup (here dominated by the thermal noise of the 50 Ω load of the isolator) and $i(f)$ the current fluctuations generated by the junction. Voltage fluctuations across the junction lead to environmental corrections to the cyclostationary third moment, in a similar way they do in the stationary regime [15,23,24]. Using circuit theory, we find the different contributions to the cyclostationary third moment of voltage fluctuations detected by the amplifier connected to the transmission line [18]:

$$K_{v,3}(f) = t(f)^3 R_J^3[K_{\mathrm{int}}(f) + K_{\mathrm{env}}(f) + K_{fb}(f)] \tag{6}$$

with K_{int} the intrinsic contribution of the sample, K_{env} the contribution due to the term $t'(f)v_{\mathrm{env}}(f)$ in Eq. (5) and K_{fb}, the contribution due to the term $i(f)Z_{\mathrm{eff}}(f)$. In Ref. [18], these quantities have been calculated at zero bias and zero frequency, i.e., neglecting the signal propagation in the circuit, which does not correspond to our experiment. In the following we derive the last two terms in Eq. (6) at any bias I_{dc} and in the case of realistic microwave setup. We have computed the contributions to the third moment due to thermal fluctuations of the environment K_{env} and the feedback effect K_{fb} using the so-called cascaded Langevin approach [15], where we use the separability of timescales between the fluctuations $\delta V(t)$ and $i(t)$.

Considering that the noise generated by the junction responds adiabatically to the applied voltage, we have:

$$\langle i(t)^2\rangle = S(V(t)) + \delta V(t)\frac{dS}{dV}\Big|_{V(t)}, \tag{7}$$

where brackets $\langle\rangle$ designate an ensemble average and $V(t) = R_J[I_{dc} + I_{ac}\cos(2\pi f_0 t)]$ is the periodically modulated bias voltage. In the following, we choose a more general approach. Because of cyclostationarity, Fourier components $i(f')$ separated by a frequency αf_0 where f_0 is the driving frequency (here $f_0 = 3f$ with f the detection frequency) and α an integer, can be correlated:

$$S_\alpha(f') = \langle i(f')i(\alpha f_0 - f')\rangle. \tag{8}$$

$S_\alpha(f')$ is the dynamical response of order $\alpha > 0$ of the noise at frequency f' to an excitation at f_0 [25]. S_0 is the static response, i.e., the photoexcited noise. On the top of the excitation at f_0, the voltage fluctuations $\delta V(f + \varepsilon)$ around

frequency f introduce additional correlations:

$$\langle i(f')i(\alpha f_0 + f + \varepsilon - f')\rangle = D_\alpha(f')\delta V(f+\varepsilon), \quad (9)$$

where $D_\alpha(f')$ is the noise susceptibility of order α. The most general correlator thus reads:

$$\langle i(f')i(f'')\rangle = \sum_{\alpha\in\mathbb{Z}} S_\alpha(f')\delta(f''+f'-\alpha f_0) + D_\alpha(f')\delta V(f''+f'-\alpha f_0). \quad (10)$$

Because of the adiabaticity, the quantities S_α and D_α are frequency independent, given by the coefficients of the Fourier series:

$$S(t) = \sum_{\alpha\in\mathbb{Z}} S_\alpha e^{i2\pi\alpha f_0 t}, \frac{dS}{dV}(t) = \sum_{\alpha\in\mathbb{Z}} D_\alpha e^{i2\pi\alpha f_0 t}. \quad (11)$$

A. Environmental thermal noise

We now evaluate the term $K_{\rm env}$ of Eq. (6), the contribution to the third moment of the noise generated by the external circuit. Due to the impedance mismatch between the junction and the measuring circuit, the voltage fluctuations propagating from the environment towards the junction are partially reflected back to the amplification chain, and the measured voltage is $v_{\rm mes}(f) = -i(f)\frac{1}{2}t(f)R_J + r(f)v_{\rm env}(f)$ with $r(f) = (Z_{\rm out}(f) - Z_0)/(Z_{\rm out}(f) + Z_0)$. The modulation by $v_{\rm env}$ of the variance of the noise generated by the junction leads to a third order correlation:

$$K_{\rm env}(f) = 3\frac{2r(f)}{t(f)R_J}\langle v_{\rm env}(f)i^2(f)\rangle. \quad (12)$$

According to Eq. (10), $\langle i^2(f)\rangle = D_1(f)\delta V(-f) = D_1(f)t'(-f)v_{\rm env}(-f)$. Since the circuit is reciprocal, $t'(-f)/t(f) = (R_J/Z_0)e^{-2i\phi}$ with ϕ the phase of $t(f)$. Introducing the spectral density of the environmental noise $\langle v_{\rm env}(f)v_{\rm env}(-f)\rangle = \frac{1}{2}k_B T_{\rm env}Z_0$ Eq. (12) becomes:

$$K_{\rm env}(f) = 3D_1 k_B T_{\rm env} r(f) e^{-2i\phi}. \quad (13)$$

To demonstrate this environmental effect experimentally, we increased the effective temperature $T_{\rm env}$ so that $K_{\rm env}$ becomes the main contribution to the measured third moment. To do so, we excited the sample with a sine wave $v_{\rm env}(t) = A\sin 2\pi(f+\varepsilon)t$ with $\varepsilon = 83$ MHz in addition to the drive at frequency $3f$. This is equivalent to an increase in the noise temperature at frequency $f+\varepsilon$ in a very narrow band. The effective $T_{\rm env}$ is estimated from the amplitude of the reflected sine wave superimposed to the measured noise. We measured the skewnesses $\langle X^3\rangle$ and $\langle P^3\rangle$ for different $I_{\rm ac}$ and $I_{\rm dc}$ and are presented in Fig. 5. One clearly observes a quantitative agreement between the measurements (symbols) and the theoretical prediction of Eq. (13), both for the dependence on $I_{\rm dc}$ (main plot in Fig. 5) and $I_{\rm ac}$ (right inset), up to an overall multiplicative factor.

B. Feedback effect

The feedback term K_{fb} in Eq. (6) represents the contribution of the junction modulating its own noise through the impedance $Z_{\rm in}$. Using Eq. (10) we calculate the feedback

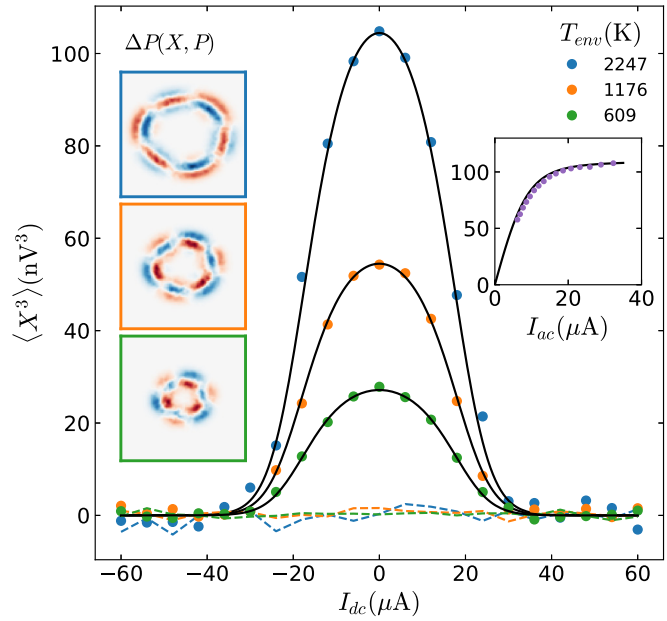

FIG. 5. $\langle X^3\rangle$ (solid circles) and $\langle P^3\rangle$ (dashed lines) for $I_{\rm ac} = 20\ \mu A$ in the presence of a tone at frequency $f + 83$ MHz of various amplitude. Black lines correspond to fit with Eq. (13). Quadratures have been rotated to maximize the signal on $\langle X^3\rangle$. Left insets: differential probability $\Delta\mathcal{P}(X,P)$ for each excitation power. Right inset: measured $\langle X^3\rangle(I_{\rm ac})$ for $I_{\rm dc} = 0$.

contribution to the three current correlation:

$$\langle i(f)i(f')i(f'')\rangle_{fb} = \sum_{\rm perm}\langle i(f)\langle i(f')i(f'')\rangle\rangle = \sum_{\substack{\rm perm,\\ \alpha\in\mathbb{Z}}} D_\alpha(f')\langle i(f)i(f'+f''-\alpha f_0)\rangle \times Z_{\rm eff}(f'+f''-\alpha f_0), \quad (14)$$

where the sum is over the cyclic permutation of frequencies f, f', and f'' with $f+f'+f'' = 3f$ as imposed by the cyclostationarity. This gives for a narrow bandwidth:

$$K_{fb}(f) = 3\sum_{\alpha\in\mathbb{Z}} D_\alpha S_{1-\alpha} Z_{\rm eff}((2-3\alpha)f). \quad (15)$$

This is a quite unexpected result: The feedback effect on the cyclostationary third moment measured in a narrow band around frequency f involves the environmental impedance not only at f but also at higher frequencies $2f$, $4f$, $5f$, etc. This is a generalization of previous derivation [18], which treated only the case $I_{\rm dc} = 0$.

At zero dc bias $I_{\rm dc} = 0$, only the term $D_1 S_0 Z_{\rm eff}(f)$ is nonzero. In contrast with the environmental contribution which is proportional to D_1 and saturates at high ac excitation, the $D_1 S_0$ term is almost linear in $I_{\rm ac}$, see insets of Fig. 6. We use this property to separate the different contributions to the skewnesses, which can be reliably fitted by $aI_{\rm ac} + bD_1(I_{\rm ac})$, with a and b real numbers (which are different for the in-phase and in-quadrature component), see Fig. 6. Besides the global gain of the measurement, $a = (K_{\rm int} + K_{fb})/I_{\rm ac}$, and $b = 3k_B T_{\rm env} r(f)$. b being known allows us to remove the

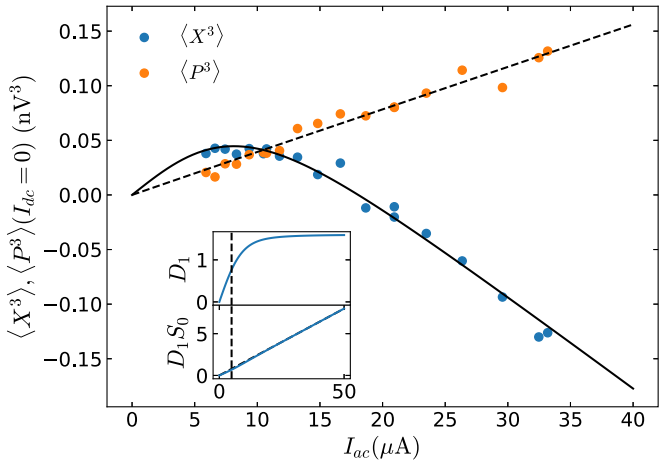

FIG. 6. Dependence of the measured third moment with ac bias I_{ac} on both in-phase and in-quadrature components. Data are fitted by $aD_1(I_{ac}) + bI_{ac}$, with $a = 1.2 \times 10^{11}$, $b = -9 \times 10^{-6}$ for $\langle X^3\rangle$ and $a = 0$, $b = 0.4 \times 10^{-6}$ for $\langle Y^3\rangle$. The global phase has been chosen to maximize contribution of K_{env} on the X component. Insets: Dependence with I_{ac} of D_1 and D_1S_0 (in arbitrary units). D_1S_0 is almost linear whereas D_1 shows a saturation for $I_{ac} \gg 2k_BT/eR_J$ (dashed line).

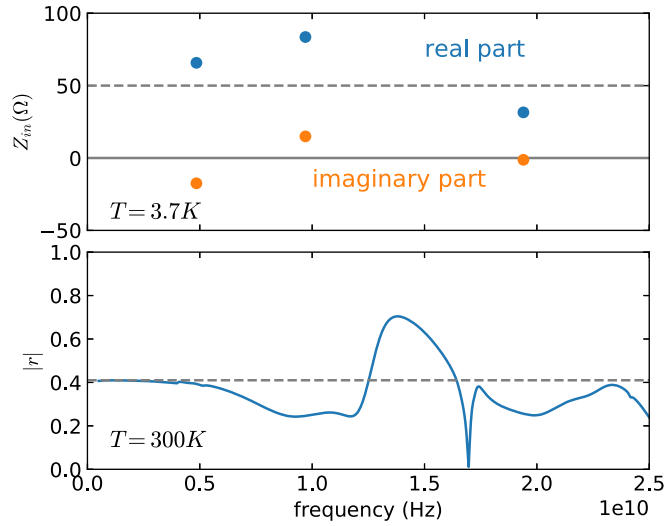

FIG. 8. Top: Input impedance Z_{in} seen by the junction, extracted from the fit of K_{fb} (circles). Bottom: Magnitude of the reflection coefficient of the sample at 300 K (solid line), measured using a vector network analyzer. The dashed line corresponds to the reflexion of a pure resistance of 116 Ω, i.e., the dc resistance of junction measured at 300 K.

K_{env} contribution from previous measurements, by subtracting $bD_1(I_{ac}, I_{dc})$ from $\langle X^3\rangle$ and $\langle P^3\rangle$ for all values of I_{dc} and I_{ac}.

We show in Fig. 7 the skewnesses of both components after subtraction of environmental contributions K_{env}. Obviously, these differ from a constant, indicating the presence of extra terms in the feedback contributions, see Eq. (15). This equation contains an infinite sum involving the environmental impedance taken at very high frequency. We expect however these contributions to decay as frequency increases because of the capacitance of the junction ($C \approx 0.2$ pF based on geometry) shunting the environmental impedance at high frequency, the cutoff being approximately given by ∼20 GHz.

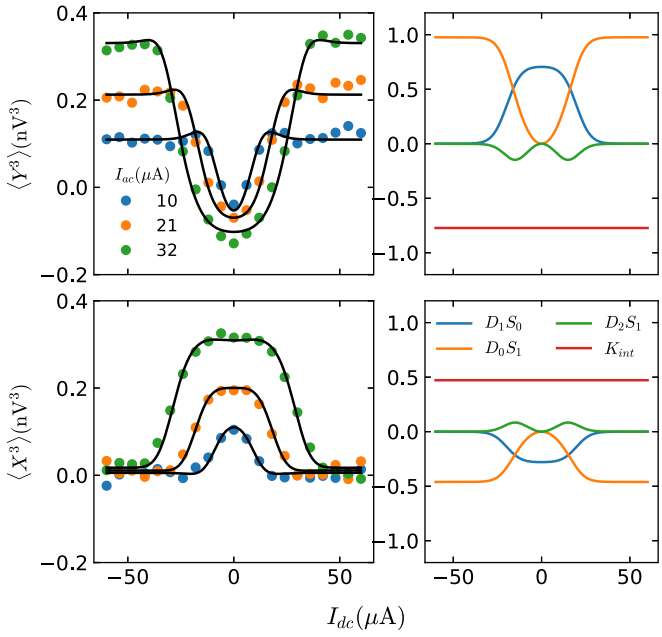

FIG. 7. Third moment of in-phase (X) and in-quadrature (P) components of voltage fluctuations after subtraction of the environmental contribution K_{env}. Graphs on the left: Dots represent data and black plain lines are the result from the fitting routine using Eq. (15) plus a constant which is attributed to the intrinsic contribution K_{int}. Graphs on the right: each contribution to $\langle X^3\rangle$ and $\langle Y^3\rangle$ for $I_{ac} = 20$ μA plotted separately.

To obtain quantitative results, we extracted the values of the environmental impedance using a fitting routine. First we determine the global gain $G(f)^3\Delta f^2$, from the magnitude of K_{env}, assuming $T_{env} = 3.7$ K and $|r| = 0.44$. Then we used a three parameter fit on the in-phase and in-quadrature component of $K_{int} + K_{fb}$, corresponding to the environmental impedances appearing in K_{fb} for $\alpha < 4$, plus one parameter for the dephasing ϕ between K_{int} and K_{env}. The fitted data are represented on Fig. 7. The fitting routine has also been performed with less parameters, by omitting for example the D_2S_1 contribution, however the obtained impedances were unrealistic.

C. Characterization of the electromagnetic environment

Our data on $\langle X^3\rangle$ and $\langle P^3\rangle$ are very well accounted for by Eq. (6) for all dc and ac excitations. This involves, beside the total gain $G(f)^3\Delta f^2$, environmental parameters: the electromagnetic response of the environment through the phase $\phi = -0.1$ rad (for K_{env}) and the impedances $Z_{in}(f)$, $Z_{in}(2f)$, and $Z_{in}(4f)$ (for K_{fb}), whose values are presented in Fig. 8.

We also show in Fig. 8 the magnitude of the reflection coefficient $|r|$ measured at room temperature with a vector network analyzer. The magnitude below 5 GHz is close to what is expected for a transmission line terminated by a simple resistor, which coincides with $Z_{in}(f)$ being close to 50 Ω. At 10 GHz, a lower reflection can indicate a better matching which coincides with $Z_{in}(2f)$ being closer to the

junction resistance. Our knowledge of the environment is however too crude to predict the value of $Z_{\text{in}}(4f)$ from $|r|$.

From this analysis, two conclusions can be drawn for future works. Because of the frequency dependence of the reactive part of $Z_{\text{eff}}(f)$ and $r(f)$, all environmental contributions cannot be projected on the in-phase component X of voltage fluctuations. Therefore, in order to extract the intrinsic third moment of the sample, both noise components X and P must be measured. Second, a careful design of the electromagnetic environment is necessary to separate the intrinsic contribution from the environmental ones. For example, by providing a low impedance environment at frequency $2f$, K_{int} becomes the dominant contribution at high dc bias.

IV. CONCLUSION

We have measured the cyclostationary third moment of current fluctuations at finite frequency $f = 4.85$ GHz in a tunnel junction photoexcited at frequency $3f$. We have observed third order correlations between the in-phase and in-quadrature components of the electric field at frequency f which depends on both the dc and ac bias. Thanks to a theoretical analysis we can decompose these correlations into three contributions: the intrinsic shot noise of the junction and its modulation by the external noise at frequency f as well as through a feedback mechanism that involves the impedance of the detection circuitry even way outside the detection bandwidth.

Our analysis paves the way towards the design of new experiments probing the third moment of current fluctuations at high frequencies. This includes, for example, the case of systems with nontrivial dynamics, like diffusive wires [11] or systems in the regime where the quantum dynamics associated with the timescale h/eV matters [25–27]. It also includes the case of high impedance samples (quantum dots, Coulomb blockaded systems, etc.) which can be matched to 50 Ω only around a single frequency f and where usual wide-band techniques fail to operate. It also opens the possibility to use quantum limited amplifiers, such as the Josephson parametric amplifier, to study non-Gaussian noise in the quantum regime. As a matter of fact, the existence of correlations similar to the one we observed but at temperatures such that $k_BT < hf$ would imply third order squeezing in the radiation emitted by a tunnel junction, as has been recently observed in superconducting parametric amplifiers [28]. We hope our work will also trigger theoretical advances, such as how to extend theories used to link quantum fluctuations of electrical current to that of the radiated electromagnetic field [29], which has proven successful to predict second order correlations that lead to squeezing but are probably insufficient to account for third order correlations.

ACKNOWLEDGMENTS

We acknowledge fruitful discussions with Edouard Pinsolle, and the technical help of G. Laliberté. This work was supported by the Canada Excellence Research Chair program, the Canada Research Chair program, the Canada First Research Excellence Fund, the NSERC, the MDEIE, the Canada Foundation for Innovation, the MDEIE, the FRQNT via the INTRIQ, the Université de Sherbrooke via the EPIQ, the CFREF via the Institut Quantique.

[1] Y. M. Blanter and M. Büttiker, Phys. Rep. **336**, 1 (2000).
[2] F. W. J. Hekking and J. P. Pekola, Phys. Rev. Lett. **96**, 056603 (2006).
[3] B. Reulet and D. E. Prober, Phys. Rev. Lett. **95**, 066602 (2005).
[4] E. Pinsolle, A. Rousseau, C. Lupien, and B. Reulet, Phys. Rev. Lett. **116**, 236601 (2016).
[5] D. Bagrets and F. Pistolesi, Phys. Rev. B **75**, 165315 (2007).
[6] Y. Bomze, G. Gershon, D. Shovkun, L. S. Levitov, and M. Reznikov, Phys. Rev. Lett. **95**, 176601 (2005).
[7] J. Gabelli and B. Reulet, Phys. Rev. B **80**, 161203(R) (2009).
[8] N. Ubbelohde, C. Fricke, C. Flindt, F. Hohls, and R. J. Haug, Nat. Commun. **3**, 612 (2012).
[9] T. Fujisawa, T. Hayashi, Y. Hirayama, H. D. Cheong, and Y. H. Jeong, Appl. Phys. Lett. **84**, 2343 (2004).
[10] K. E. Nagaev, S. Pilgram, and M. Büttiker, Phys. Rev. Lett. **92**, 176804 (2004).
[11] S. Pilgram, K. E. Nagaev, and M. Büttiker, Phys. Rev. B **70**, 045304 (2004).
[12] A. V. Galaktionov, D. S. Golubev, and A. D. Zaikin, Phys. Rev. B **68**, 235333 (2003).
[13] B. Reulet, J. Senzier, and D. E. Prober, Phys. Rev. Lett. **91**, 196601 (2003).
[14] E. Pinsolle, S. Houle, C. Lupien, and B. Reulet, Phys. Rev. Lett. **121**, 027702 (2018).
[15] C. W. J. Beenakker, M. Kindermann, and Y. V. Nazarov, Phys. Rev. Lett. **90**, 176802 (2003).
[16] J. Gabelli, L. Spietz, J. Aumentado, and B. Reulet, New J. Phys. **15**, 113045 (2013).
[17] J. Gabelli and B. Reulet, J. Stat. Mech.: Theory Exp. (2009) P01049.
[18] T. T. Heikkilä and L. Roschier, Phys. Rev. B **71**, 085316 (2005).
[19] L. Spietz, K. W. Lehnert, I. Siddiqi, and R. J. Schoelkopf, Science **300**, 1929 (2003).
[20] G. B. Lesovik and L. S. Levitov, Phys. Rev. Lett. **72**, 538 (1994).
[21] R. J. Schoelkopf, A. A. Kozhevnikov, D. E. Prober, and M. J. Rooks, Phys. Rev. Lett. **80**, 2437 (1998).
[22] L. S. Levitov and M. Reznikov, Phys. Rev. B **70**, 115305 (2004).
[23] B. Reulet, J. Gabelli, L. Spietz, and D. E. Prober, *Perspectives of Mesoscopic Physics* (World Scientific, Singapore, 2010), pp. 211–221.
[24] M. Kindermann, Y. V. Nazarov, and C. W. J. Beenakker, Phys. Rev. B **69**, 035336 (2004).
[25] J. Gabelli and B. Reulet, Phys. Rev. Lett. **100**, 026601 (2008).
[26] K. Thibault, J. Gabelli, C. Lupien, and B. Reulet, Phys. Rev. Lett. **114**, 236604 (2015).
[27] J. Gabelli and B. Reulet, Proc. SPIE **6600**, 66000T (2007).
[28] C. W. Sandbo Chang, C. Sabín, P. Forn-Díaz, F. Quijandría, A. M. Vadiraj, I. Nsanzineza, G. Johansson, and C. M. Wilson, Phys. Rev. X **10**, 011011 (2020).
[29] A. L. Grimsmo, F. Qassemi, B. Reulet, and A. Blais, Phys. Rev. Lett. **116**, 043602 (2016).